Evaluation of an explanted porcine skin model to investigate infection with the dermatophyte *Trichophyton rubrum*

Fritz Ka-Ho Ho, M. Begoña Delgado-Charro, and Albert Bolhuis*

Department of Pharmacy and Pharmacology, University of Bath, Bath BA2 7AY, United Kingdom

*Corresponding author: email: a.bolhuis@bath.ac.uk, phone +44 (0)1225 383813

Abstract

Dermatophytosis is a fungal infection of skin, hair and nails, and the most frequently found causative agent is *Trichophyton rubrum*. The disease is very common and often recurring, and it is therefore difficult to eradicate. To develop and test novel treatments, infection models that are representative of the infection process are desirable. Several infection models have been developed, including the use of cultured cells, isolated corneocytes, explanted human skin, or reconstituted human epidermis. However, these have various disadvantages, ranging from not being an accurate reflection of the site of infection, as is the case with e.g. cultured cells, to being difficult to scale up or having ethical issues (e.g. explanted human skin). We therefore sought to develop an infection model using explanted porcine skin, which is low cost and ethically neutral. We show that in our model, fungal growth is dependent on the presence of skin, and adherence of conidia is time-dependent with maximum adherence observed after ~2 hours. Scanning electron microscopy suggested the production of fibril-like material that links conidia to each other and to skin. Prolonged incubation of infected skin leads to luxurious growth and invasion of the dermis, which is not surprising as the skin is not maintained in conditions to keep the tissue alive, and therefore is likely to lack an active immune system that would limit fungal growth. Therefore, the model developed seems useful to study the early stages of infection. Furthermore, we demonstrate that the model can be used to test novel treatment regimens for tinea infections.

Introduction

Dermatophytosis is a highly prevalent superficial fungal infection that can affect skin, nails and hair. It affects an estimated 20-25% of the world's population (1), and the worldwide expenditure on antifungal agents to treat dermatophytosis is estimated at 2.5 billion USD. Risk factors include participation in sports activities, type 2 diabetes, and aging (2), and because of the latter two, the prevalence of dermatophytosis is expected increase further. The disease is generally mild, but it does impact the quality of life. However, in diabetics it contributes to the severity of the diabetic foot (3) and in immunocompromised patients the disease can be more severe and even life-threatening (4).

Worldwide, the most common causative agent of dermatophytosis is the anthropophilic fungus *Trichophyton rubrum* (5). This organism and other dermatophytes are able to invade keratinised tissues where they obtain nutrients by degrading the keratin, a main component of hair, the stratum corneum of the skin, and the nail plate. The disease is normally transmitted by contact with infected dead skin, nail or hair particles containing hyphae or spores called arthroconidia (6). *In vitro*, *Trichophyton* spp. often form microconidia, which are small pyriform spores that form along the sides of hyphae. These spores are not observed *in vivo*, but both arthro- and microconidia from related *Trichophyton* spp. (*T. interdigitale* and *T. metagrophytes*) are infective and show similar levels of adherence to corneocytes (7, 8).

To study the infection process of skin, a number of infection models have been developed. These include the use of isolated corneocytes (7, 8), explanted human skin (9-12), cell cultures using Chinese Hamster Ovary (CHO) cells (13) or immortal human keratinocytes (HaCaT cells) (14), and reconstituted human epidermis (RHE) (15). With some of these models, such as those based on cell cultures, it is unclear how relevant they are to the initial stages of infection as there is no skin structure and a lack of the stratum corneum. This

problem is partially solved by using RHE grown on polycarbonate culture inserts, but RHE still lacks an integrated dermis and has a significantly higher permeability compared to human skin (16, 17). Explanted human skin does not have these issues, but sourcing human tissue can be challenging, costly and is complicated by ethical issues. Our aim in this study was to evaluate the feasibility of using an explanted porcine skin model, which is relatively simple and affordable. We have previously used a porcine skin model for bacterial infections (18), and an important advantage of this model is that it is ethically neutral as the tissue can be obtained from the abattoir as surplus material from pigs that go into the food chain. Also, porcine skin is a well-established model for transdermal and topical delivery of drugs and has proved to be very useful in pre-clinical stages of research as it is very similar to human skin with similar thickness and hair density (19). Here we show that porcine skin is useful to study the early stages of infection and can be used to evaluate the treatment with antifungals.

Materials and methods

Cultures and growth conditions

Trichophyton rubrum ATCC 28188, obtained from Fisher Scientific (Loughborough, UK) was routinely grown on potato dextrose agar (Sigma-Aldrich, St. Louis, MO, USA) for 15 days at 30°C to induce full sporulation. Microconidia were harvested with sterile water containing 1% Tween-20 (Fisher Scientific), washed and resuspended in sterile water, and stored at -20°C until use. The freezing process does not lead to a significant reduction in viability of conidia but longer storage does (20), and to ensure consistent viability of inocula, aliquots were used within two weeks of freezing.

Extracellular protease activity

Keratin was isolated from human hair (obtained from a local hairdresser) as described (21), and after dialysis against water was adjusted to a concentration of 20 mg/mL keratin. This was diluted 10-fold in potato dextrose broth (PDB) or minimal salts medium (50 mM $NH_4H_2PO_4$, 5.75 mM K_2HPO_4, 3.4 mM KH_2PO_4, 2 mM $CaCl_2$ and 0.25% glucose; pH 5.2), which was then inoculated with *T. rubrum* conidia to a final concentration of 5 x 10^2 conidia/mL. Cultures (1.5 mL each) were then grown for 10 days in 24-well plates at 30ºC. Mycelium was removed by centrifugation, and the supernatant retained for protease activity assays using azocasein as described (22).

Porcine skin sterilisation

Porcine skin was sourced from a local abattoir. The skin was obtained from 3-month old gilts (female, approximately 60 kg) of the Large White breed. Skin from two animals was used; results on skin obtained from one animal were similar to those from the second animal. Full thickness skin was obtained, and the skin was then stored at 4ºC. The next day, the skin was

dermatomed to a thickness of 750 µm and stored frozen until use. To avoid damage to the skin, it was not submitted to any cleansing process at the abattoir such as scalding with hot water to remove hair, neither before nor following harvesting it from the animal, and was simply rinsed with water at the laboratory before being dermatomed. On the day of the experiment, dorsal skin samples were defrosted at room temperature and cut in approximately 1 cm^2 square pieces. The hair on the skin was removed with scissors and the skin was washed three times in sterile phosphate buffered saline (PBS). Next, the porcine skin was sterilised with chlorine gas as described (23) with minor modifications. Briefly, the skin pieces were placed in a Petri dish, which was then put in a chamber with chlorine gas that was generated by mixing 20 mL glacial acetic acid (VWR, Fontenay-sous-Bois, France) and 10 mL sodium hypochlorite solution (10-15%, Sigma-Aldrich) in a beaker. The skin was sterilised with chlorine gas at room temperature for 15 minutes on an orbital platform shaker at 15 rpm, after which the skin was turned around and incubated for a further 15 min in the chlorine gas. After the treatment, the skin was rinsed twice with sterile PBS, followed by washing by being placed in a tube with 10 mL sterile PBS for 30 mins on a shaker at 200 rpm. The skin pieces were then transferred onto minimal salts agar plates (50 mM $NH_4H_2PO_4$, 5.75 mM K_2HPO_4, 3.4 mM KH_2PO_4, 2 mM $CaCl_2$ and 0.25% glucose; pH 5.2) for 30 minutes before experiments were continued.

Adherence to porcine skin

Time-dependent adherence of *T. rubrum* to the stratum corneum (SC) of porcine skin was determined by measuring the number of conidia that did or did not adhere. To this purpose, 10 µL of *T. rubrum* conidia (1×10^4 colony forming units (CFU)/mL) was pipetted on the top of sterilised porcine skin that was placed on minimal salts agar, followed by incubation for 0-24 hours at 30°C. After incubation, the skin pieces were washed with 1 mL sterile PBS and

the number of conidia that did not adhere to the skin was measured by a viable plate count of the wash on Sabouraud dextrose agar (SDA). To measure the number of conidia that adhered to the skin, washed skin pieces were incubated with Trypsin-EDTA (0.25%) (Gibco, Paisley, UK) for 15 mins at 37°C on shaker at 220 rpm, followed by viable plate counting.

Adherence to HaCaT cells

HaCaT cells (24) were plated at a density of 1×10^5 cells per well in 24-well tissue culture plates, cultured in 1 mL Dulbecco's Modified Eagle Medium (DMEM; Sigma-Aldrich)) supplemented with 10% fetal bovine serum and penicillin-streptomycin (10,000 U/mL). The HaCaT cells were incubated at 37°C and 5% CO_2 for 3 days to reach confluence. The medium was replaced by DMEM, without fetal bovine serum and antibiotics, the night before inoculation. 5 µL of *T. rubrum* conidia (1×10^5 CFU/mL) was added into each well and incubated for 0-24 hours at 37°C and 5% CO_2.

To measure the number of conidia not adhered to the HaCaT cells, the supernatant was collected and the CFU of *T. rubrum* were determined on SDA. To measure the number of conidia adhered to the HaCaT cells, the DMEM solution in the well was removed and the wells were washed 3 times in PBS. 0.5 mL of Trypsin-EDTA (0.25%) was added followed by incubation for 5 to 10 minutes at 37°C. Once the cells detached, 0.5 mL of DMEM solution was added to the well and cells were resuspended. The solution was transferred to SDA plates for a viable cell count.

Histology staining

To study the effect of chlorine gas to the structure of the skin after sterilising, specimens were fixed overnight at 4°C in 10% neutral-buffered formalin. To cryoprotect the tissues, specimens were immersed in 30% sucrose (Sigma-Aldrich) in PBS until the tissue sank, followed by

freezing the sample in Optimal Cutting Temperature compound (OCT; CellPath, Powys, UK) using dry ice methanol slurry. Samples were then cryosectioned and stained using haematoxylin (Gill No.3; Sigma-Aldrich) and eosin (BDH, Poole, UK), then mounted with DPX mountant (Sigma-Aldrich) and imaged using light microscopy (Zeiss Axioscope).

To visualise the infection process, sterilised porcine skin was placed on minimal salts agar and inoculated with 10 µL of *T. rubrum* conidia (1×10^5 CFU/mL), followed by incubation for 0-72 hours at 30°C. The skin was fixed with 10% neutral buffered formalin overnight at 4°C, then the fixed specimens were dehydrated, embedded in paraffin and sectioned. The sections were deparaffinised, and then stained using a periodic acid-schiff-diastase (PAS-D) staining kit (Sigma-Aldrich) following the manufacturer's instructions, and samples were observed using light microscopy.

Field Emission Scanning Electron Microscopy

All specimens were treated with the same procedures as outlined in histopathology section. After the treatment, the specimens were fixed in 2.5% glutaraldehyde in 0.1 M sodium cacodylate buffer (pH 7.3) overnight, followed by post-fixing with 1% osmium tetroxide for 2 h. This was followed by rinsing three times in sodium cacodylate buffer (pH 7.3) for 10 minutes. The specimens were dehydrated in a graded acetone series (10, 30, 50, 70, 80, 90, 95 and 100%) for 15 minutes per change. After that, the specimens were mounted onto a SEM plug and coated with chromium. The samples were then imaged using FESEM (JSM 6301F, JEOL, Tokyo, Japan).

Antifungal susceptibility testing

Explanted porcine skin was sterilised and infected with conidia as above, with the porcine skin placed on mineral salts agar. This was incubated for 3 days at 30°C to induce fungal skin infection. The infected skin was then treated topically using clinically used antifungal creams, being 1% clotrimazole (Bayer, Reading, UK) or 1% terbinafine hydrochloride (GlaxoSmithKline, Brentford, UK). Both were applied as directed in the patient information leaflets. In brief, the creams were applied thinly on the skin (using a sterile swab) once per day (terbinafine) or twice per day (clotrimazole), for a period of 7 days. The explanted skin was kept at 30°C for the duration of the experiment and was rinsed once per day with sterile PBS to simulate washing. Control specimens were treated the same but were wiped with a sterile swab dipped in sterile water instead of with antifungal cream. After one week, all specimens were washed with sterile PBS and gently dried with sterile tissue paper. The specimens were then transferred to fresh mineral salts agar and incubated for a further 7 days at 30°C.

Statistical analysis

The results were represented as the mean ± standard deviation (SD). The mean differences between two groups of data was analysed by a repeated measures analysis of the variance (ANOVA). The data were considered statistically significant with a *p*-value off less than 0.05.

Results

Keratinases are important virulence factors for dermatophytes, as these degrade the keratin in skin, nail or hair that these organisms thrive on (25). We firstly sought to identify conditions in which these enzymes are secreted by *T. rubrum*. In a nutritionally rich medium (PDB), production of extracellular protease activity was very low, also when it was supplemented

with keratin. In contrast, significantly more proteolytic activity was found in culture supernatant when *T. rubrum* was grown in minimal salts medium containing keratin (Supplementary Figure 1). There was no fungal growth in the absence of keratin (not shown), demonstrating that in these conditions the growth of *T. rubrum* is dependent on the keratin. This medium was therefore used in the porcine skin infection model.

When testing fungal growth on porcine skin, it became clear that it was important to sterilise the skin first, as otherwise there was a lot of bacterial growth. Initially we tested surface disinfection with 70% ethanol, but that did not stop bacterial growth (not shown). Also, ethanol can be damaging to skin as it selectively extracts lipids from the stratum corneum (26, 27). However, sterilisation with chlorine gas did not damage skin as described before (23) and observed by histology staining (Supplementary Figure 2), while this treatment was sufficient to prevent bacterial growth on the porcine skin.

A schematic of the infection model, in which dermatomed porcine skin, on a polycarbonate membrane, is placed on top of minimal salts agar, is shown in Fig 1A. When conidia were inoculated on the porcine skin, growth of *T. rubrum* was observed after several days of growth at 30ºC (Fig 1B). Similar to the growth in liquid medium, this was dependent on the presence of skin, as the fungi were unable to grow on minimal salts agar without porcine skin (Fig 1C).

The adherence of conidia observed in this explanted porcine skin was compared to a previously established *in vitro* model using HaCaT cells, an immortal line of keratinocytes (24). Using these two approaches we measured the number of conidia that adhered to skin (Fig 2A). With porcine skin, maximum adherence was reached within 2 hours, while that

218 took ~3 hours with HaCaT cells. A repeated measures ANOVA on those first three hours
219 showed that these differences were not significant. The adherence of conidia was mirrored by
220 the number of non-adherent conidia (Fig 2B). However, the number of non-adherent conidia
221 continued to drop to less than 5%, while the number of adherent conidia did not increase
222 beyond 60% of the number of conidia initially applied.
223
224 To visualise the infection process, we performed histology analysis of infected porcine skin.
225 These are shown in Fig 3, with examples of the features described below indicated with
226 arrows. Also, the position of the stratum corneum, epidermis and dermis is indicated in Fig
227 3A. After 3 hours incubation (Fig 3A), conidia can be observed above the stratum corneum,
228 while after 6 hours (Fig 3B) some conidia appear to be embedded in the stratum corneum.
229 Development of germ tubes, the first step in the formation of a mycelium, can be observed
230 after 9 hours (Fig 3C). Upon longer incubation of the infected skin samples, mycelium can be
231 observed after 24 hours, and hyphae can be seen in the stratum corneum (Fig 3D), while after
232 48 hours the stratum corneum was damaged and sometimes absent (Fig 3E). After 72 hours
233 (Fig 3E), the epidermis also appeared damaged and degraded, and there was clearly invasion
234 of the dermis by *T. rubrum*.
235
236 To get a more detailed view at the infection process, samples were prepared for SEM
237 imaging. In these images, microconidia were easily recognised with their characteristic
238 piriform shape. Sometimes after 3 hours (Fig 4A), but more frequently after 6 hours (Fig 4B),
239 fibril-like material that appeared to connect the conidia was observed. Longer incubation, at
240 9-12 hours (Fig 4C and D) showed conidia also connecting to the skin. After 24 hours,
241 conidia could be observed that appeared completely embedded in the skin with a fibrous film
242 (Fig 4E), while hyphae were also present (Fig 4F and G). After 48 hours (Fig 4H) the skin

was mostly covered in mycelium. It should be noted that some of the images show that the conidial preparation does contain some hyphal fragments as seen in Fig 4A and B, but in all experiments the percentage of microconidia was at least 90%.

The porcine skin model was further tested using antifungal creams that are commonly used for the topical treatment of tinea infections. These were 1% terbinafine hydrochloride and 1% clotrimazole, which were both used as directed in the patient information leaflet on infected porcine skin. The skin was rinsed once per day – to mimic washing – and kept at 30°C for the duration of the experiment, a temperature that closely matches that of skin in feet and hands (28, 29). After treatment for a week, the explanted skin was washed, dried and incubated for a further 7 days at 30°C. As shown in Fig 5, the control (without antifungal) was fully covered with mycelium whereas no *T. rubrum* was visible on the skin that was treated with the antifungal creams, showing successful treatment of the infected skin with the topical products.

Discussion

As we have shown here, explanted porcine skin is a useful model system to monitor the infection process by dermatophytes such as *T. rubrum*. Porcine skin was chosen as its structure is very similar to that of human skin, including a similar thickness of the stratum corneum, epidermis, and dermis, and a comparable hair density (19, 30). A difference is a thicker layer of subcutaneous layer of fat in pigs and possibly differences in the immune system (30), but here only dermatomed skin was used. Because of these similarities, pig skin is considered a suitable model for e.g. wound healing, toxicology and dermal delivery of drugs, also since the flux of drugs through porcine skin is within the same order of magnitude

as that for human skin (17). In contrast, skin from e.g. rodents is very different, with significantly higher hair density, a much thinner epidermis and dermis, and higher permeability of drugs (17, 30). Domestic pigs do not suffer often from dermatophytosis, but they are sometimes infected with the zoonotic species *Trichophyton mentagrophytes* (31). Furthermore, while the related species *T. rubrum* is considered anthropophilic, it occasionally causes infections in animals such as dogs (32), while the species has also been used in rodent models of infection (33). Thus, even though there are no reported cases of pigs being infected with *T. rubrum*, the above does suggest that porcine skin is a suitable model to study infections with this species.

In dermatophytes, extracellular proteases have important roles in nutrient acquisition, invasion (25) and, for some specific proteases, adherence (11). While we have not tested which specific proteases are expressed, we have shown that proteolytic activity can be detected *in vitro* in minimal salts medium containing keratin, while this activity is absent in a rich medium containing keratin. Similarly, we showed that fungal growth on plates with minimal salts agar only occurs when porcine skin is present. This minimal salts medium does contain a carbon source (glucose), but no nitrogen source, and fungal growth on porcine skin is therefore likely to be dependent on the release of nitrogen-containing compounds that are obtained by proteolytic degradation of the keratin in skin. Previous studies have also shown that these proteases are expressed when nutrients are limiting and proteins such as keratin are present (34).

Maximum adherence to the porcine skin was achieved within 2 hours, which compared well to a previously published *in vitro* model using keratinocytes (14), for which we found maximum adherence within 3 hours. We did not make a comparison with other models as it

was not our aim to comprehensively contrast and compare these with the porcine skin model. Moreover, the keratinocyte model using HaCaT cells is a very simple epidermal model, but it was nevertheless useful to make this comparison as, firstly, this model has been used previously as a model for *T. rubrum* infection (14) and, secondly, HaCat cells are very frequently used in skin research.

Adherence has also been measured using corneocytes, which are terminally differentiated keratinocytes that form most of the stratum corneum. Zurita and Hay (8) showed that maximum adherence of *Trichophyton interdigitale* to corneocytes occurred within 3-4 hours. Similarly, Aljabre *et al* (7) showed time-dependent increase in adherence of conidia to corneocytes of both *T. interdigitale* and *T. mentagrophytes* over a 6-hour period. It should however be noted that in the studies with keratinocytes or isolated corneocytes, adherence was measured with cells immersed in liquid, rather than on intact skin exposed to air. Furthermore, those models lack a stratum corneum and other skin structures, although it is unclear whether that would affect the adherence.

It was noted that the number of conidia that adhered did not rise above ~50-60% of the number of conidia applied with both models, while the number of non-adherent conidia continued to decrease over at least a 6-hour period. This suggests that either the conidia lose their viability, or that the conidia adhere so strongly that they can no longer be removed. The latter may indeed be the case, as SEM revealed formation of fibril-like material between adjacent conidia within 6 hours, and between conidia and the stratum corneum in 9 hours. After 24 hours, some conidia appeared completely embedded in the stratum corneum, and it is conceivable that this leads to a strong interaction, making them difficult to remove. Similar fibrils have also been observed with *T. mentagrophytes* microconidia (10) and arthroconidia

(12) when grown on explanted human skin, and both of these studies found indeed a strong adherence of the conidia to the skin. Our results for *T. rubrum* are consistent with these previous findings. The fibril-like material could consist of the same material as the extracellular matrix (ECM) of *T. rubrum* biofilms, which was shown to be rich in polysaccharides (35), but at present the nature of the fibril-like material is unknown and their role in attachment is purely speculative.

Adherence of conidia is followed by invasion of the skin, in which formation of germ tubes plays an important role. We observed germ tubes within 9 hours, which is similar to what has been observed *in vitro* (36). Penetration of hyphae into the skin was observed with histology staining and light microscopy after 24 hours. This penetration was not observed with SEM, but this technique will only visualise the surface which will make it more difficult to identify hyphae that penetrate into the skin. Development of mycelium occurred after 24 hours, while longer incubation (48-72 hours) resulted in the skin being completely covered by a fungal mat, damage of the epidermis, and invasion of the dermis. Such luxuriant growth and invasion are not observed *in vivo*, but deeper tissues can be affected in immunocompromised patients (37-39). Indeed, the immune system has an important role in restricting the growth of dermatophytes to dead keratinised tissue only (40). However, the skin used in this study is not kept alive after harvesting, and is simply stored dry at 4^{o}C, dermatomed the next day, and then stored at -20^{o}C. Although we have not tested this, it is unlikely to contain an active immune system, thus explaining the invasion of the epidermis and dermis. We also do not observe lesions as observed *in vivo* or with a human skin infection model in which the skin is kept alive (41), which again may be a consequence of using porcine skin that is not kept viable.

In summary, we have tested the feasibility of a porcine skin infection model to study dermatophytosis and treatment strategies. The successful treatment with creams commonly used for fungal skin infections demonstrates that the model is also suitable to test novel strategies for prevention and treatment of fungal skin infections. The infection model is relatively simple, cheap and ethically neutral as the porcine skin is obtained from slaughterhouse material. When compared to other models such as cultured keratinocytes, the model also has the advantage that it contains a complete skin structure comprising stratum corneum, epidermis and dermis. Reconstituted human epidermis does contain a stratum corneum but lacks a dermis and is more permeable to drugs as compared to intact skin (16). This might suggest that also fungal invasion would be influenced, but there is no evidence for this at present. Furthermore, we have only made a comparison with the keratinocyte model and have not determined which model is a better reflection of a fungal skin infection. Whilst explanted human skin has been used in other studies (9-12, 41), sourcing human skin can be costly and complicated by ethical issues. It is important to note that porcine skin is very similar to human skin, with a similar thickness and hair density, and even when stored frozen the barrier function of the stratum corneum is well preserved (17, 19). Importantly, it behaves similarly to human skin with respect to penetration of drugs, and porcine skin is therefore an important model to study dermal delivery or drugs. Indeed, as shown here the porcine model can also be used to analyse topical treatment with antifungals, albeit that in this case the data are only qualitative as we did not test different dosages. A limitation of our model is the lack of an immune system, resulting in invasion of the dermis and more luxuriant growth than would be observed *in vivo*. Therefore, late stages of infection as well as chronic infections cannot be modelled well with this approach. However, we believe the model is very useful to study in particular the early stages of infection, and we are currently planning to identify

367 virulence factors involved. Moreover, the model can be used to test novel regimes to prevent
368 or treat fungal skin infections.
369

Compliance with Ethical Standards

Conflict of interest

The authors declare that they have no conflicts of interest.

Ethical Approval

Ethical approval for the study was obtained from the relevant ethics committees. Porcine skin was collected from a local slaughterhouse, and no experimental procedures were performed on live animals.

References

1. Havlickova B, Czaika VA, Friedrich M. Epidemiological trends in skin mycoses worldwide. Mycoses. 2008;51 Suppl 4:2-15.
2. Elewski BE, Tosti A. Risk factors and comorbidities for onychomycosis: Implications for treatment with topical therapy. J Clin Aesthet Dermatol. 2015;8(11):38-42.
3. Gupta AK, Humke S. The prevalence and management of onychomycosis in diabetic patients. Eur J Dermatol. 2000;10(5):379-84.
4. Rouzaud C, Hay R, Chosidow O, Dupin N, Puel A, Lortholary O, et al. Severe dermatophytosis and acquired or innate immunodeficiency: A Review. J Fungi (Basel). 2015;2(1):4.

5. Nenoff P, Kruger C, Ginter-Hanselmayer G, Tietz HJ. Mycology - an update. Part 1: Dermatomycoses: causative agents, epidemiology and pathogenesis. J Dtsch Dermatol Ges. 2014;12(3):188-209.

6. Yazdanparast SA, Barton RC. Arthroconidia production in *Trichophyton rubrum* and a new *ex vivo* model of onychomycosis. J Med Microbiol. 2006;55(Pt 11):1577-81.

7. Aljabre SH, Richardson MD, Scott EM, Rashid A, Shankland GS. Adherence of arthroconidia and germlings of anthropophilic and zoophilic varieties of *Trichophyton mentagrophytes* to human corneocytes as an early event in the pathogenesis of dermatophytosis. Clin Exp Dermatol. 1993;18(3):231-5.

8. Zurita J, Hay JH. Adherence of dermatophyte microconidia and arthroconidia to human keratinocytes *in vitro*. J Invest Dermatol. 1987;89(5):529-34.

9. Smijs TG, Bouwstra JA, Schuitmaker HJ, Talebi M, Pavel S. A novel *ex vivo* skin model to study the susceptibility of the dermatophyte *Trichophyton rubrum* to photodynamic treatment in different growth phases. J Antimicrob Chemother. 2007;59(3):433-40.

10. Duek L, Kaufman G, Ulman Y, Berdicevsky I. The pathogenesis of dermatophyte infections in human skin sections. J Infect. 2004;48(2):175-80.

11. Băguţ ET, Baldo A, Mathy A, Cambier L, Antoine N, Cozma V, et al. Subtilisin Sub3 is involved in adherence of *Microsporum canis* to human and animal epidermis. Vet Microbiol. 2012;160(3-4):413-9.

12. Kaufman G, Horwitz BA, Duek L, Ullman Y, Berdicevsky I. Infection stages of the dermatophyte pathogen *Trichophyton*: microscopic characterization and proteolytic enzymes. Med Mycol. 2007;45(2):149-55.

13. Esquenazi D, Souza W, Sales Alviano C, Rozental S. The role of surface carbohydrates on the interaction of microconidia of *Trichophyton mentagrophytes* with epithelial cells. FEMS Immunol Med Microbiol. 2003;35(2):113-23.

14. Bitencourt TA, Macedo C, Franco ME, Assis AF, Komoto TT, Stehling EG, et al. Transcription profile of *Trichophyton rubrum* conidia grown on keratin reveals the induction of an adhesin-like protein gene with a tandem repeat pattern. BMC Genomics. 2016;17:249.

15. Faway E, Cambier L, Mignon B, Poumay Y, Lambert de Rouvroit C. Modeling dermatophytosis in reconstructed human epidermis: A new tool to study infection mechanisms and to test antifungal agents. Med Mycol. 2017;55(5):485-94.

16. Zghoul N, Fuchs R, Lehr CM, Schaefer UF. Reconstructed skin equivalents for assessing percutaneous drug absorption from pharmaceutical formulations. ALTEX. 2001;18(2):103-6.

17. Schmook FP, Meingassner JG, Billich A. Comparison of human skin or epidermis models with human and animal skin in in-vitro percutaneous absorption. Int J Pharm. 2001;215(1-2):51-6.

18. Alhusein N, Blagbrough IS, Beeton ML, Bolhuis A, De Bank PA. Electrospun Zein/PCL fibrous matrices release tetracycline in a controlled manner, killing *Staphylococcus aureus* both in biofilms and *ex vivo* on pig skin, and are compatible with human skin cells. Pharm Res. 2016;33(1):237-46.

19. Herkenne C, Naik A, Kalia YN, Hadgraft J, Guy RH. Pig ear skin *ex vivo* as a model for *in vivo* dermatopharmacokinetic studies in man. Pharm Res. 2006;23(8):1850-6.

20. Ho FKH, Delgado-Charro B, Bolhuis A. A microtiter plate-based quantitative method to monitor the growth rate of dermatophytes and test antifungal activity. J Microbiol Methods. 2019;165:105722.

21. Nakamura A, Arimoto M, Takeuchi K, Fujii T. A rapid extraction procedure of human hair proteins and identification of phosphorylated species. Biol Pharm Bull. 2002;25:569-572

441 22. Bolhuis A, Koetje E, Dubois JY, Vehmaanpera J, Venema G, Bron S, et al. Did the
442 mitochondrial processing peptidase evolve from a eubacterial regulator of gene expression?
443 Mol Biol Evol. 2000;17:198-201.
444 23. Yang Q, Phillips PL, Sampson EM, Progulske-Fox A, Jin S, Antonelli P, et al.
445 Development of a novel *ex vivo* porcine skin explant model for the assessment of mature
446 bacterial biofilms. Wound Repair Regen. 2013;21(5):704-14.
447 24. Boukamp P, Petrussevska RT, Breitkreutz D, Hornung J, Markham A, Fusenig NE.
448 Normal keratinization in a spontaneously immortalized aneuploid human keratinocyte cell
449 line. J Cell Biol. 1988;106(3):761-71.
450 25. Vermout S, Tabart J, Baldo A, Mathy A, Losson B, Mignon B. Pathogenesis of
451 dermatophytosis. Mycopathologia. 2008;166(5-6):267-75.
452 26. Bommanan D, Potts RO, Guy RH. Examination of the effect of ethanol on human
453 stratum corneum in vivo using infrared spectroscopy. J Control Release. 1991; 16:299-304
454 27. Kwak S, Brief E, Langlais D, Kitson N, Lafleur M, Thewalt J.
455 Ethanol perturbs lipid organisation in models of stratum corneum membranes: an
456 investigation combining differential scanning calorimetry, infrared and (2)H NMR
457 spectroscopy. Biochem Biophys Acta. 2012;1818: 1410-1419
458 28. Petrova NL, Whittam A, MacDonald A, Ainarkar S, Donaldson AN, Bevans J, et al.
459 Reliability of a novel thermal imaging system for temperature assessment of healthy feet. J
460 Foot Ankle Res. 2018;11:22.
461 29. Shilco P, Roitblat Y, Buchris N, Hanai J, Cohensedgh S, Frig-Levinson E, et al.
462 Normative surface skin temperature changes due to blood redistribution: A prospective study.
463 J Therm Biol. 2019;80:82-8.
464 30. Summerfield A, Meurens M, Ricklin ME. The immunology of the porcine skin and its
465 value as a model for human skin. Mol Immunol. 2015;66:14-21

466 31. Jackson PGG, Cockcroft, PD. Handbook of pig medicine 2007. London, Saunders
467 Elsevier
468 32. Van Rooij P, Declerq J, Beguin H. Canine dermatophytosis caused by *Trichophyton*
469 *rubrum*: an example of man-to-dog transmission. Mycoses. 55:e15-e17
470 33. Matos Baltazar L, Assis Santos D. Perspective of animal models of dermatophytosis
471 caused by *Trichophyton rubrum.* Virulence. 2015;6:372-375
472 34. Apodaca G, McKerrow JH. Regulation of *Trichophyton rubrum* proteolytic activity.
473 Infect Immun. 1989;57(10):3081-90.
474 35. Costa-Orlandi CB, Sardi JC, Santos CT, Fusco-Almeida AM, Mendes-Giannini MJ.
475 *In vitro* characterization of *Trichophyton rubrum* and *T. mentagrophytes* biofilms.
476 Biofouling. 2014;30(6):719-27.
477 36. Liu T, Zhang Q, Wang L, Yu L, Leng W, Yang J, et al. The use of global
478 transcriptional analysis to reveal the biological and cellular events involved in distinct
479 development phases of *Trichophyton rubrum* conidial germination. BMC Genomics.
480 2007;8:100.
481 37. Smith KJ, Welsh M, Skelton H. *Trichophyton rubrum* showing deep dermal invasion
482 directly from the epidermis in immunosuppressed patients. Br J Dermatol. 2001;145(2):344-
483 8.
484 38. Kim SH, Jo IH, Kang J, Joo SY, Choi JH. Dermatophyte abscesses caused by
485 *Trichophyton rubrum* in a patient without pre-existing superficial dermatophytosis: a case
486 report. BMC Infect Dis. 2016;16:298.
487 39. Nir-Paz R, Elinav H, Pierard GE, Walker D, Maly A, Shapiro M, et al. Deep infection
488 by *Trichophyton rubrum* in an immunocompromised patient. J Clin Microbiol.
489 2003;41(11):5298-301.

40. Ogawa H, Summerbell RC, Clemons KV, Koga T, Ran YP, Rashid A, et al. Dermatophytes and host defence in cutaneous mycoses. Med Mycol. 1998;36 Suppl 1:166-73.

41. Corzo-Leon DE, Munro CA, MacCallum DM. An *ex vivo* human skin model to study superficial fungal infections. Front Microbiol. 2019;10:1172.

497 Figures

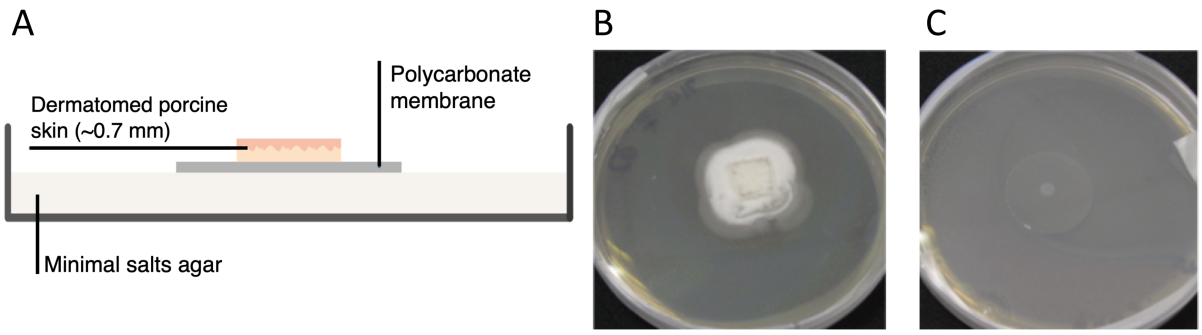

498

499 **Fig 1. Explanted porcine skin infection model.** (A) Schematic of the setup used for the

500 infection model. (B) Fungal growth on explanted porcine skin, 7 days after inoculation with

501 conidia. No growth is observed in the absence of porcine skin (C).

502

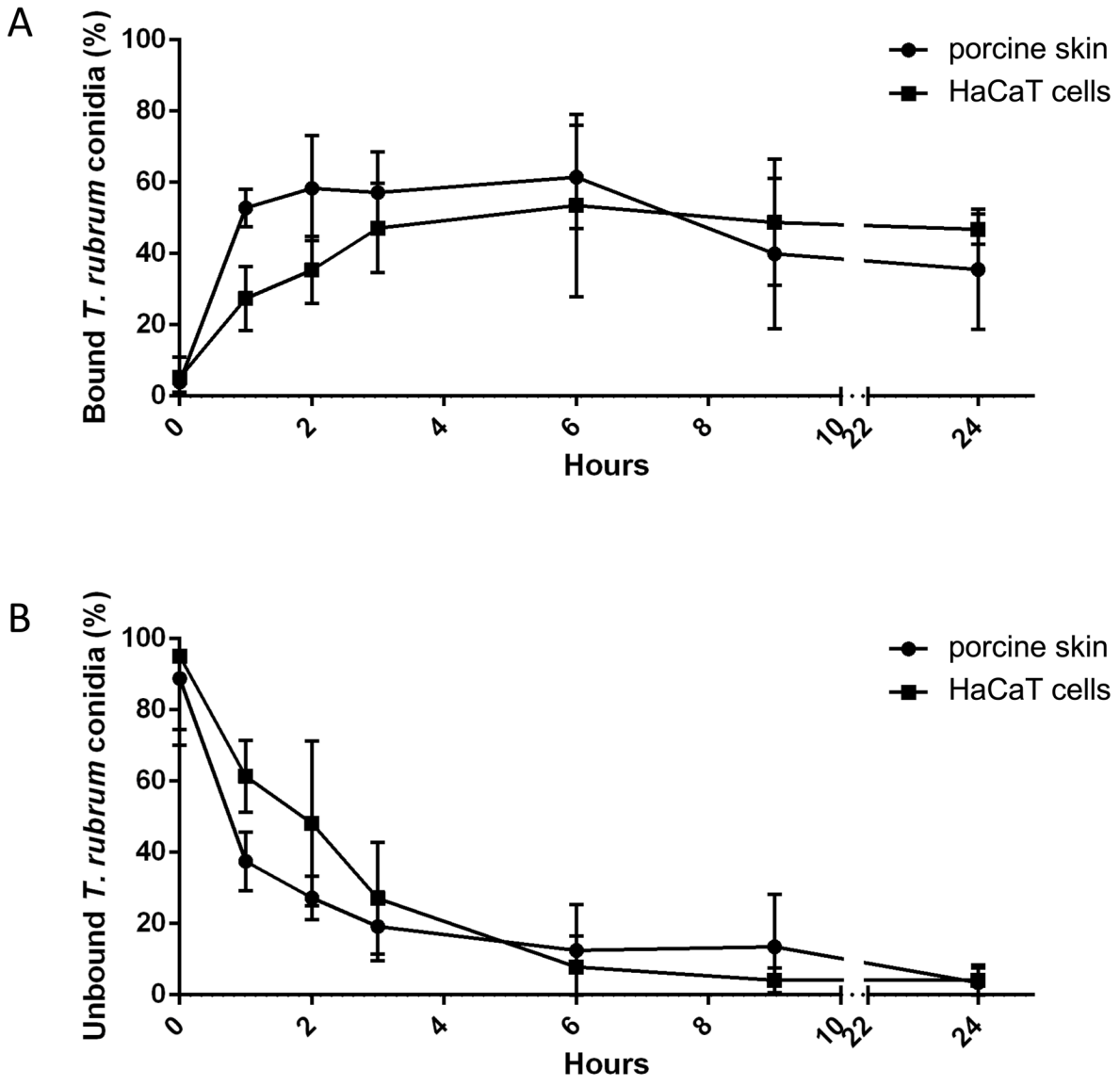

503

504

505

506 **Fig 2. Measurement of *T. rubrum* conidia bound (A) and unbound (B) to porcine skin**

507 **and HaCaT cells between 0 and 24 hours.** There is a reverse relationship between bound

508 and unbound conidia in both models, as they showed an increase of conidial adherence with a

509 decrease in non-adherent conidia (data derived from 2-3 independent experiments, with 3-6

510 repeats per experiment).

511

512

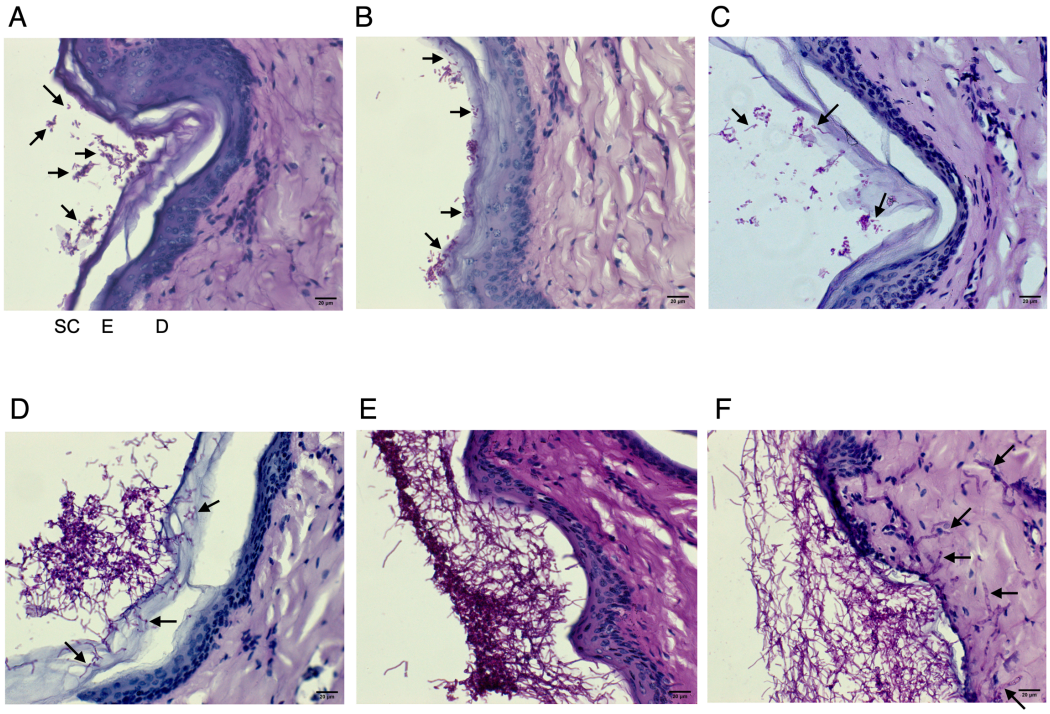

513

514 **Fig 3. Histopathological analysis of infected porcine skin.** Explanted porcine skin was
515 infected with *T. rubrum* conidia, incubated for 3 hours (A), 6 hours (B), 9 hours (C), 24 hours
516 (D), 48 hours (E) and 72 hours (F). After incubation, samples were prepared for PAS-D
517 staining and visualised using light microscopy. Features described in the main text are
518 indicated with arrows. In A, the position of the stratum corneum (SC), epidermis (E) and
519 dermis (D) is indicated. Scale bar = 20 μm.

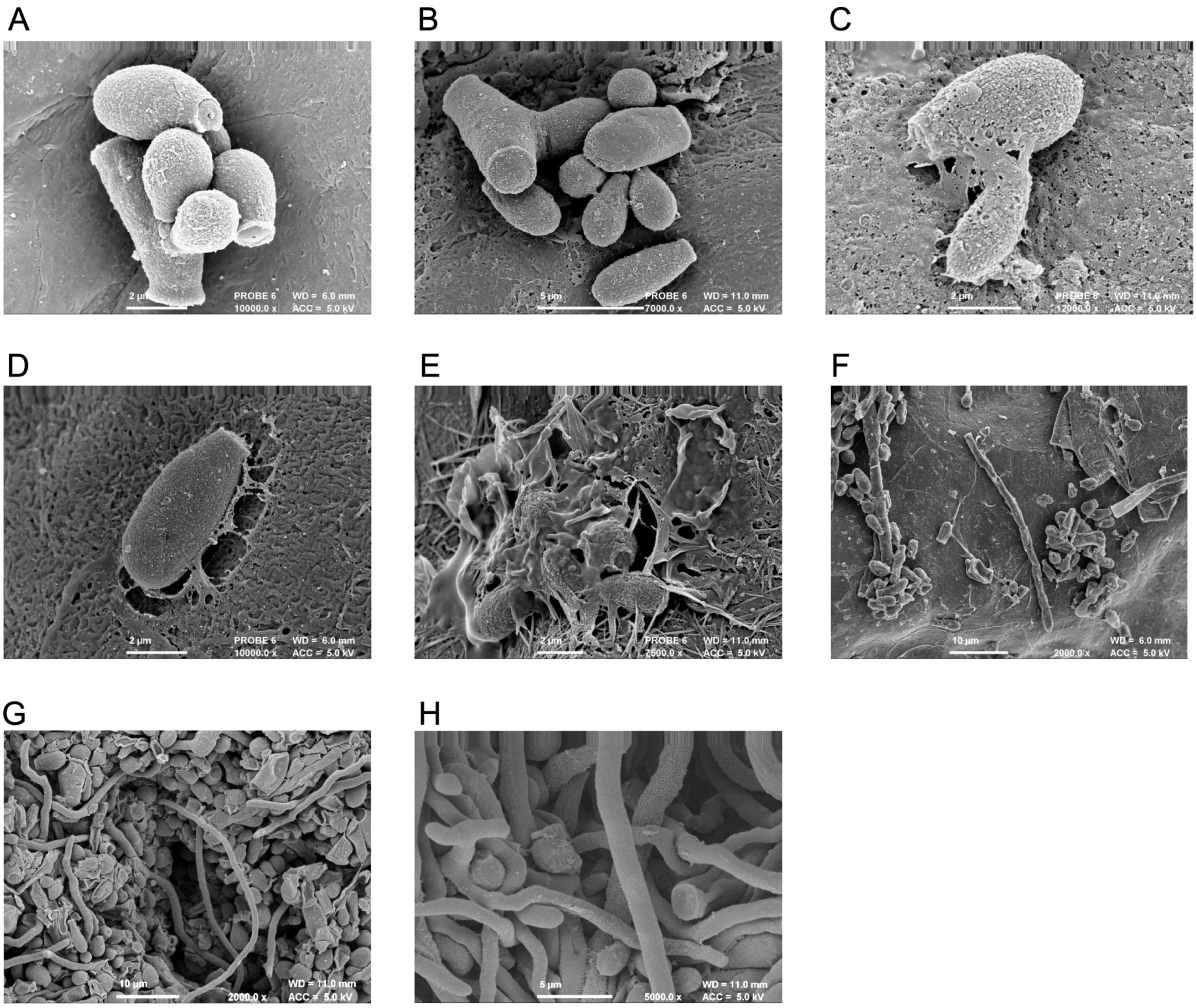

520

521

522 **Fig 4. Electron microscopy analysis of infected porcine skin.** Explanted porcine skin was
523 infected with *T. rubrum* conidia, incubated for 3 hours (A), 6 hours (B), 9 hours (C), 12 hours
524 (D), 24 hours (E-G) and 48 hours (H), followed by visualisation using FESEM. Different
525 magnifications were used depending on the features that were visualised. Scale bars shown
526 are 2 µm, except for B (5 µm), F (10 µm) and G (5 µm).

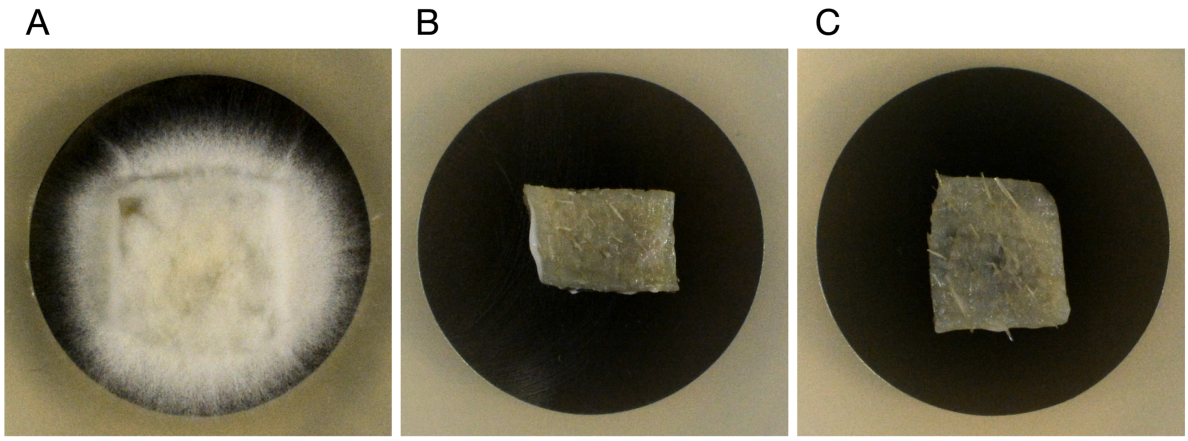

Fig 5. Topical treatment of infected porcine skin. Explanted porcine skin was infected with *T. rubrum* conidia and incubated for 3 days at 30ºC. After this the skin, which was kept at 30ºC on minimal salts agar, was treated daily for a period of 7 days with water (control, A), 1% clotrimazole (B), or 1% terbinafine hydrochloride (C). Treatment was as directed in the patient information leaflet, and the skin was also rinsed daily to simulate washing. After treatment, the skin was washed and incubated for a further 7 days at 30ºC.

Supplementary figures

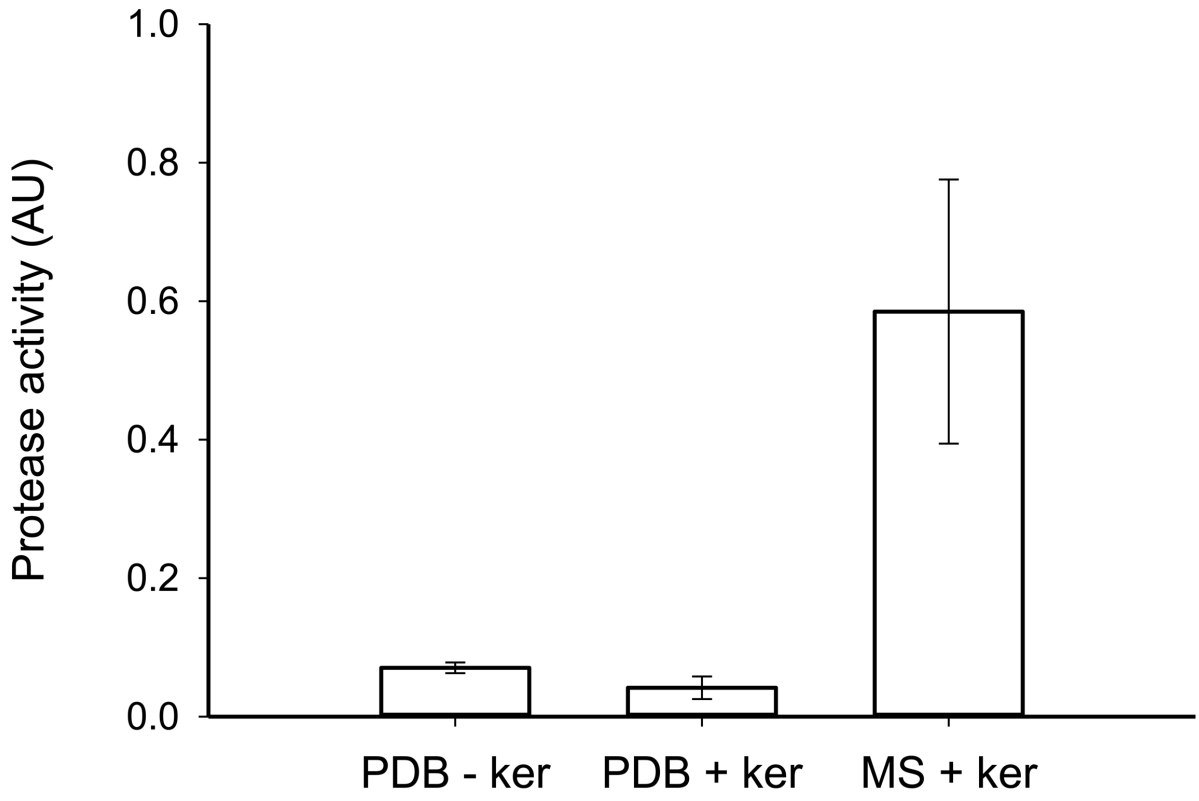

Supplementary Fig 1. Proteolytic activity in the culture supernatant. *T. rubrum* was grown for 10 days in rich medium (PDB) or minimal salts medium (MS) in the presence or absence of 0.2% keratin (+/- ker). Proteolytic activity, which is expressed in arbitrary units (AU), was then determined using azocasein. Error bars indicate standard deviation of the mean from three independent experiments.

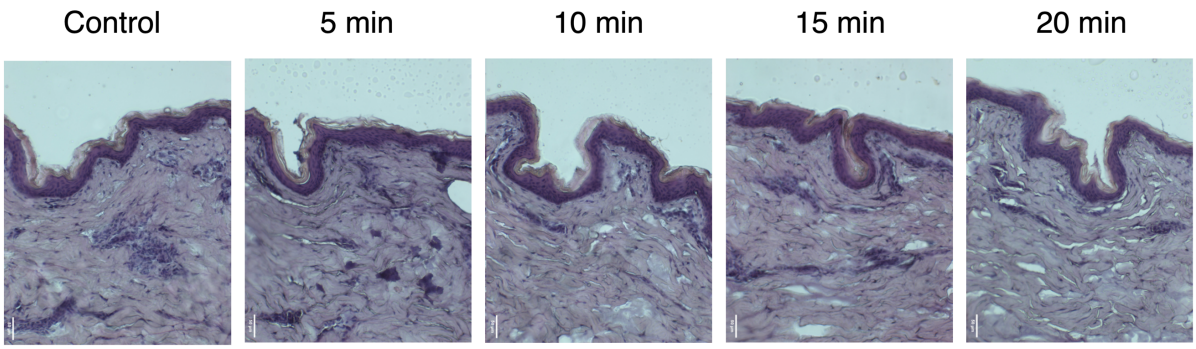

Supplementary Figure 2. Skin samples were treated on each side with chlorine gas with the times indicated. Specimens were then fixed, cryoprotected, and stained with haemotoxylin/eosin, and imaged using light microscopy. The scale bars indicated are 50 µm.